
Why Regularized Auto-Encoders learn Sparse Representation?

Devansh Arpit, Yingbo Zhou, Hung Ngo, Venu Govindaraju

Department of Computer Science

SUNY Buffalo

Buffalo, NY 14260

{devansha, yingbozh, hungngo, govind}@buffalo.edu

Abstract

Although a number of auto-encoder models enforce sparsity explicitly in their learned representation while others don't, there has been little formal analysis on what encourages sparsity in these models in general. Therefore, our objective here is to formally study this general problem for regularized auto-encoders. We show that both regularization and activation function play an important role in encouraging sparsity. We provide sufficient conditions on both these criteria and show that multiple popular models—like De-noising and Contractive auto-encoder— and activations—like Rectified Linear and Sigmoid—satisfy these conditions; thus explaining sparsity in their learned representation. Our theoretical and empirical analysis together, throws light on the properties of regularization/activation that are conducive to sparsity. As a by-product of the insights gained from our analysis, we also propose a new activation function that overcomes the individual drawbacks of multiple existing activations (in terms of sparsity) and hence produces performance at par (or better) with the best performing activation for all auto-encoder models discussed.

1 Introduction

Both Sparse Representation (SR) and Neural Network (NN) are biologically inspired [12, 26, 27, 9] models used heavily in machine learning [21, 15, 5]. A key commonality between these models is finding distributed representation [13, 11] for observed data although the former focuses on finding sparse distributed representation while the latter focuses on learning complex functions. When combined together, some of the main advantages of sparse distributed representation in the context of deep neural networks [1] has been shown to be information disentangling and manifold flattening [2], and better linear separability and representational power [7].

For these reasons, our objective in this paper is to investigate why a number of regularized Auto-Encoders (AE) learn sparse representation. AEs are specially interesting for this matter because of the clear distinction between their learned *encoder* representation and *decoder* output. This is in contrast with other deep models where there is no clear distinction between the encoder and decoder parts. The idea of AEs learning SR is not new. Due to the aforementioned biological connection between SR and NNs, a natural follow-up pursued by a number of researchers was to propose AE variants that encouraged sparsity in their learned representation [19, 14, 25, 22]. On the other hand, there has also been work on empirically analyzing/suggesting the sparseness of hidden representations learned after pre-training with unsupervised models [23, 20, 24]. However, there has been no prior work on formally analyzing why regularized auto-encoders learn sparse representation in general, to the best of our knowledge. The main challenge behind doing so is the analysis of non-linear, and even worse, non-convex objective functions. In addition, questions regarding the efficacy of activation functions and the choice of regularization on AE objective are often raised since there are multiple available choices for both. We also try to address these questions in regards with SR in this paper.

We address these problems in two parts. We first provide sufficient conditions on AE regularizations that encourage low pre-activations in hidden units. We then analyze the properties of activation functions that coupled with such regularizations result in sparse representation and find that multiple popular activations have these desirable properties. Finally the second part shows multiple popular AE objectives including De-noising auto-encoder (DAE) [32] and Contractive auto-encoder (CAE) [29] indeed have the suggested form of regularization; thus explaining why existing AEs encourage sparsity in their latent representation. Based on our theoretical analysis, we empirically study multiple popular AE models and activation functions in order to analyze their behaviour in terms of sparsity in the learned representations. Besides confirming our analysis, these experiments also serve to illustrate a comparative performance of these AE models and activation functions. Thus our analysis provides novel tools that can be used for both, comparing existing AEs under the same hood, as well as predicting the behavior of (new) regularizations and activation functions (in terms of sparsity) leading to a deeper understanding of AEs.

2 Auto-Encoders and Sparse Representation

Auto-Encoders (AE) [30, 3] are a class of single hidden layer neural networks that minimize the data reconstruction error while learning an intermediate mapping between the input and output space. An auto-encoder consists of two parts – an encoder and a decoder. An input ($\mathbf{x} \in \mathbb{R}^n$) is first mapped to the latent space by an encoder function $f_e : \mathbb{R}^n \rightarrow \mathbb{R}^m$ given by $\mathbf{h} := f_e(\mathbf{x}) = s_e(\mathbf{W}\mathbf{x} + \mathbf{b}_e)$ where \mathbf{h} is the hidden representation vector, s_e is the encoder activation function, $\mathbf{W} \in \mathbb{R}^{m \times n}$ is the weight matrix, and \mathbf{b}_e is the encoder bias. Then we map the hidden output back to the original space by a decoder function $f_d : \mathbb{R}^m \rightarrow \mathbb{R}^n$ given by $\mathbf{y} = f_d(\mathbf{h}) = s_d(\mathbf{W}^T\mathbf{h} + \mathbf{b}_d)$ where \mathbf{y} is the reconstructed counterpart of \mathbf{x} , s_d is the decoder activation function, \mathbf{b}_d is the decoder bias. The objective of a basic auto-encoder is to minimize the following with respect to $\{\mathbf{W}, \mathbf{b}_e, \mathbf{b}_d\}$

$$\mathcal{J}_{AE} = \mathbb{E}_{\mathbf{x}}[\ell(\mathbf{x}, f_d(f_e(\mathbf{x})))] \quad (1)$$

where $\ell(\cdot)$ is a loss function. The motivation behind this objective is to capture predominant repeating patterns in data. Thus even though the auto-encoder optimization learns to map an input back to itself, the focus is on learning a noise invariant representation (manifold) of data.

2.1 Part I: What encourages *sparsity* during Auto-Encoder training?

Learning a dictionary adapted to a set of training data such that the latent code is sparse is generally formulated as the following optimization problem [26]

$$\min_{\mathbf{W}, \mathbf{h}} \sum_{i=1}^N \|\mathbf{x}_i - \mathbf{W}^T \mathbf{h}_i\|^2 + \lambda \|\mathbf{h}_i\|_1 \quad (2)$$

The above optimization is convex in each one of \mathbf{W} and \mathbf{h} when the other is fixed and hence this objective is generally solved alternately in each variable while fixing the other. Note that ℓ^1 penalty is the driving force in the above objective and forces the latent variable to be sparse. In this section we will analyze the factors that encourage sparsity in the case of AEs. For our analysis, we will use linear decoding function which addresses the more general case of continuous real valued data distributions. We will now show that both regularization as well as activation function play an important role for achieving sparsity.

Proposition 1. *Let $\{\mathbf{W}^t \in \mathbb{R}^{m \times n}, \mathbf{b}_e^t \in \mathbb{R}^m\}$ be the parameters of a regularized auto-encoder ($\lambda > 0$)*

$$\mathcal{J}_{RAE} = \mathcal{J}_{AE} + \lambda \mathcal{R}(\mathbf{W}, \mathbf{b}_e) \quad (3)$$

at training iteration t with regularization term $\mathcal{R}(\mathbf{W}, \mathbf{b}_e)$, activation function $s_e(\cdot)$ and define pre-activation $a_j^t = \mathbf{W}_j^t \mathbf{x} + b_{e_j}^t$ (thus $h_j^t = s_e(a_j^t)$). If $\frac{\partial \mathcal{R}}{\partial b_{e_j}} > 0$, where $j \in \{1, 2, \dots, m\}$, and $\mathbb{E}_{\mathbf{x}}[\mathbf{x}] = \mathbf{0}$, then updating $\{\mathbf{W}^t, \mathbf{b}_e^t\}$ along the negative gradient of $\lambda \mathcal{R}$, results in $\mathbb{E}_{\mathbf{x}}[a_j^{t+1}] < \mathbb{E}_{\mathbf{x}}[a_j^t]$ and $\text{var}[a_j^{t+1}] \leq \lambda_x^2 \|\mathbf{W}_j^{t+1}\|^2$ for all $t \geq 0$. Here λ_x^2 denotes the maximum eigenvalues of $\mathbb{E}_{\mathbf{x}}[\mathbf{x}\mathbf{x}^T]$.

The above proposition gives a general *sufficient* condition on regularizations for forcing the average pre-activation value ($\mathbb{E}[a_j^t]$) to go on reducing every training iteration. Of course in practice, gradients from both regularization and loss function are used. Hence in the practical version, the

interpretation of the above proposition is that as long as the gradient of the objective with respect to \mathbf{b}_e is dominated by the regularization term— thus $\partial \mathcal{J}_{RAE} / \partial b_{e_j} \geq 0$ (*strong bias gradient*), the expected value of pre-activation (a_j^t) over the data distribution goes on reducing for every hidden unit (h_j^t) with iteration t . As we will see in a bit, this is a sparsity inducing property. For the sake of concreteness, we will now analyze the bias gradient resulting from AE squared loss function. This gradient is given by:

$$\partial \ell / \partial b_{e_j} = 2 \mathbb{E}_{\mathbf{x}} [(\mathbf{b}_d + \mathbf{W}^T s_e(\mathbf{W}\mathbf{x} + \mathbf{b}_e) - \mathbf{x})^T \mathbf{W}_j \cdot \partial s_e(a_j) / \partial a_j] \quad (4)$$

Note the absolute value of first derivative of most activation functions is upper bounded (usually at most 1). Also, the optimal value of $\mathbf{b}_d = \mathbb{E}_{\mathbf{x}}[\mathbf{x} - \mathbf{W}^T \mathbf{h}]$ at every iteration. Suppose we assume the weight lengths are upper bounded and we only consider monotonically increasing $s_e(\cdot)$ with finite negative saturation. Then coupled with the natural implicit assumption on bounded length data distribution, there will exist a set of λ values for which the bias gradient from \mathcal{R} outweighs that from \mathcal{J}_{AE} for any finite valued initialization of \mathbf{b}_e . For all following iterations the bias value is always non-increasing and hence the value of s_e will be bounded because of being monotonically increasing with finite negative saturation. Thus the value of $\partial \mathcal{J}_{AE} / \partial b_{e_j}$ is upper bounded independent of the regularization coefficient λ as long as its value is chosen from the aforementioned set. This shows that the dominance of $\partial \mathcal{R} / \partial b_{e_j}$ on $\partial \mathcal{J}_{RAE} / \partial b_{e_j}$ can be controlled by the choice of λ . Intuitively higher values of λ should lead to lower average pre-activation; *however, the last argument may not strictly be true in practice due to non-linearities in the regularization* (see experiments in section 4.2 and 4.3). Finally, the upper bound on weight vectors' length can easily be guaranteed¹ using *Max-norm Regularization* or *Weight Decay* which are widely used tricks while training deep networks [10]. In the prior case every weight vector is simply constrained to lie within an ℓ^2 ball ($\|\mathbf{W}_j\|_2 \leq c \forall j \in \{1, 2, \dots, m\}$, where c is a fixed constant) after every gradient update.

Corollary 1. *If s_e is a monotonically increasing activation function and $\mathbb{E}_{\mathbf{x}}[\mathbf{x}] = \mathbf{0}$, then updating $\{\mathbf{W}^t, \mathbf{b}_e^t\}$ along the negative gradient of $\mathcal{R} = \sum_{j=1}^m f(\mathbb{E}_{\mathbf{x}}[h_j])$, results in $\mathbb{E}_{\mathbf{x}}[a_j^{t+1}] \leq \mathbb{E}_{\mathbf{x}}[a_j^t]$ and $\text{var}[a_j^{t+1}] \leq \lambda_x^2 \|\mathbf{W}_j^{t+1}\|^2$ for all $t \geq 0$. Here λ_x^2 denotes the maximum eigenvalues of $\mathbb{E}_{\mathbf{x}}[\mathbf{x}\mathbf{x}^T]$ and $f(\cdot)$ is any monotonically increasing function.*

Corollary 2. *If $s_e(\cdot)$ is a monotonically increasing convex activation function and $\mathbb{E}_{\mathbf{x}}[\mathbf{x}] = \mathbf{0}$, then updating $\{\mathbf{W}^t, \mathbf{b}_e^t\}$ along the negative gradient of $\mathcal{R} = \mathbb{E}_{\mathbf{x}} \left[\sum_{j=1}^m \left(\left(\frac{\partial h_j}{\partial a_j} \right)^q \|\mathbf{W}_j^t\|_2^p \right) \right]$, $q \in \mathbb{N}$, $p \in \mathbb{W}$, results in $\mathbb{E}_{\mathbf{x}}[a_j^{t+1}] \leq \mathbb{E}_{\mathbf{x}}[a_j^t]$ and $\text{var}[a_j^{t+1}] \leq \lambda_x^2 \|\mathbf{W}_j^{t+1}\|^2$ for all $t \geq 0$. Here λ_x^2 denotes the maximum eigenvalues of $\mathbb{E}_{\mathbf{x}}[\mathbf{x}\mathbf{x}^T]$.*

The above corollaries show that specific regularizations encourage the pre-activation of hidden units in auto-encoders towards zero values on average across the data distribution, with assumptions made only on activation function and distribution mean. We will show in section 2.2 that multiple existing AEs have regularizations of the form above.

2.1.1 Which Activation functions are good for Sparse Representation?

The above analysis in general suggests that monotonically increasing convex activation functions encourage lower expected pre-activation for both corollaries. Also note that a reduction in the expected pre-activation value ($\mathbb{E}[a_j^t]$) does not necessarily imply a reduction in the hidden unit value (h_j^t) and thus sparsity. However, these regularizations become immediately useful if we consider activation functions with negative saturation at 0, *i.e.*, $\lim_{a \rightarrow -\infty} s_e(a) = 0$. Now a lower average pre-activation value directly implies higher sparsity!

Before proceeding, we would like to mention that although the general notion of sparsity in AEs entails majority of units are de-activated, *i.e.*, their value is less than a certain threshold (δ_{\min}), in practice, a representation that is *truly sparse* (large number of hard zeros) usually yields better performance [7, 33, 34]. We will keep this in mind during our discussion.

Theorem 1. *Let p_j^t denote a lower bound of $\Pr(h_j^t \leq \delta_{\min})$ at iteration t and $s_e(\cdot)$ be a monotonically increasing function. Extending the argument of proposition 1, if $\|\mathbf{W}_j^t\|_2$ is upper bounded independent of λ then $\exists S \subseteq \mathbb{R}^+$ and $\exists T_{\min} \in \mathbb{N}$ such that $p_j^{t+1} \geq p_j^t \forall \lambda \in S, T_{\min} \leq t \leq T_{\max}$ for any fixed $T_{\max} \in \mathbb{N}$.*

¹In practice the weight lengths remain bounded from the regularized objective itself and so it is not imperative to apply this trick.

The above theorem shows usage of monotonically increasing activation functions lead to a higher probability of de-activated hidden units. This result coupled with the property $\lim_{a \rightarrow -\infty} s_e(a) = 0$ implies the average sparsity of hidden units keeps increasing after a sufficient number of iterations (T_{\min}) for such activations. On the other hand, the condition $\|\mathbf{W}_j^t\|_2$ be upper bounded is a straightforward result of applying common tricks like *Max-norm Regularization* or *Weight Decay* and hence does not undermine our result. Notice that convexity in $s_e(\cdot)$ is only desired for regularizations in corollary 2. Thus in summary, monotonically increasing convex $s_e(\cdot)$ ensure $\partial\mathcal{R}/\partial b_{e_j} \geq 0$ for regularizations in corollary 1 and 2, which in turn encourages low expected pre-activation. This finally leads to higher sparsity if $\lim_{a \rightarrow -\infty} s_e(a) = 0$.

Notice we considered strict inequality ($\partial\mathcal{R}/\partial b_{e_j} > 0$) in proposition 1 (and hence in theorem 1) even though the corollaries suggest monotonically increasing convex activations imply the relaxed case ($\partial\mathcal{R}/\partial b_{e_j} \geq 0$). This is done for two reasons: a) ensure sparsity monotonically increases for iterations $T_{\min} \leq t \leq T_{\max}$, b) $\partial\mathcal{R}/\partial b_{e_j} = 0$ is unlikely for activations with non-zero first/second derivatives because the term \mathcal{R} (above corollaries) depends on the entire data distribution.

The most popular choice of activation functions are ReLU, Maxout[8], Sigmoid, Tanh and Softplus. Maxout and Tanh are not applicable to our framework as they do not satisfy the negative saturation property.

ReLU: It is a monotonically increasing convex function; thus both corollary 1 and 2 apply. Note ReLU does not have a second derivative². Thus, in practice, this may lead to poor sparsity for the regularization in corollary 2 due to lack of bias gradients from the regularization, i.e. $\partial\mathcal{R}/\partial b_{e_j} = 0$. On the flip side, the advantage of ReLU is that it enforces hard zeros in the learned representations.

Softplus: It is also a monotonically increasing convex function and hence in general encourages sparsity for the suggested AE regularizations. In contrast to ReLU, Softplus has positive bias gradients (hence better sparsity for corollary 2) because of its smoothness. On the other hand, note that Softplus does not produce hard zeros due to asymptotic left saturation at 0.

Sigmoid: While Corollary 1 applies unconditionally to Sigmoid, corollary 2 doesn't apply in general. However, we empirically found that the majority of Sigmoid hidden units were either close to 0 or in the linear region (see experiments in section 4.1). In other words, AEs only use the convex part of Sigmoid function, which empirically supports $\mathbb{E}_{\mathbf{x}}[\partial^2 h_j / \partial a_j^2] \geq 0$ for practical purposes. This suggests Sigmoid should encourage sparsity for regularization even in corollary 2.

In conclusion, while Maxout and Tanh do not satisfy the negative saturation property at 0 and hence do not guarantee sparsity, all others– ReLU, Softplus and Sigmoid– have properties (at least in principle) that encourage sparsity in learned representations for the suggested regularizations.

2.2 Part II: Do existing Auto-Encoders learn Sparse Representation?

At this point, a natural question to ask is whether existing AEs learn Sparse Representation. To complete the loop, we show that most of the popular AE objectives have regularization term similar to what we have proposed in corollary 1 and 2 and thus they indeed learn sparse representation.

2.2.1 De-noising Auto-Encoder (DAE)

DAE [32] aims at minimizing the reconstruction error between every sample \mathbf{x} and the reconstructed vector using its corresponding corrupted version $\tilde{\mathbf{x}}$. The corrupted version $\tilde{\mathbf{x}}$ is sampled from a conditional distribution $p(\tilde{\mathbf{x}}_i | \mathbf{x}_i)$. The usual choices for this distribution are additive Gaussian and independent Bernoulli (multiplicative masking). The original DAE objective is given by

$$\mathcal{J}_{DAE} = \mathbb{E}_{\mathbf{x}} \left[\mathbb{E}_{p(\tilde{\mathbf{x}}|\mathbf{x})} [\ell(\mathbf{x}, f_d(f_e(\tilde{\mathbf{x}})))] \right] \quad (5)$$

where $p(\tilde{\mathbf{x}}_i | \mathbf{x})$ denotes the conditional distribution of $\tilde{\mathbf{x}}$ given \mathbf{x} . Since the above objective is analytically intractable due to the corruption process, we take a second order Taylor's approximation of the DAE objective³ around the distribution mean $\mu_{\mathbf{x}} = \mathbb{E}_{p(\tilde{\mathbf{x}}|\mathbf{x})} [\tilde{\mathbf{x}}]$ in order to overcome this difficulty,

Theorem 2. *Let $\{\mathbf{W}, \mathbf{b}_e\}$ represent the parameters of a DAE with squared loss, linear decoding, and i.i.d. Gaussian corruption with zero mean and σ^2 variance, at any point of training over data sampled from distribution \mathcal{D} . Let $a_j := \mathbf{W}_j \mathbf{x} + b_{e_j}$ so that $h_j = s_e(a_j)$ corresponding to sample*

²In other words, $\partial^2 h_j / \partial a_j^2 = \delta(\mathbf{W}_j \mathbf{x} + b_{e_j})$, where $\delta(\cdot)$ is the Dirac delta function. Although strictly speaking, $\partial^2 h_j / \partial a_j^2$ is always non-negative, this value is zero everywhere except when the argument is exactly 0, in which case it is $+\infty$

³As a note, even though we derive this equivalent form of DAE, we use explicit corruption for experiments.

$\mathbf{x} \sim \mathcal{D}$. Then,

$$\begin{aligned} \mathcal{J}_{DAE} = \mathcal{J}_{AE} + \sigma^2 \mathbb{E}_{\mathbf{x}} \left[\sum_{j=1}^m \left(\left(\frac{\partial h_j}{\partial a_j} \right)^2 \|\mathbf{W}_j\|_2^4 \right) + \sum_{\substack{j,k=1 \\ j \neq k}}^m \left(\frac{\partial h_j}{\partial a_j} \frac{\partial h_k}{\partial a_k} (\mathbf{W}_j^T \mathbf{W}_k)^2 \right) \right] \\ + \sum_{i=1}^n \left((\mathbf{b}_d + \mathbf{W}^T \mathbf{h} - \mathbf{x})^T \mathbf{W}^T \left(\frac{\partial^2 \mathbf{h}}{\partial \mathbf{a}^2} \odot \mathbf{W}^i \odot \mathbf{W}^i \right) \right) + o(\sigma^2) \end{aligned} \quad (6)$$

where $\frac{\partial^2 \mathbf{h}}{\partial \mathbf{a}^2} \in \mathbb{R}^m$ is the element-wise 2^{nd} derivative of \mathbf{h} w.r.t. \mathbf{a} and \odot is element-wise product.

The first term of the above regularization is of the form stated in corollary 2. Even though the second term doesn't have the exact suggested form, it is straight forward to see that this term generates non-negative bias gradients for monotonically increasing convex activation functions. Note the last term depends on the reconstruction error which practically becomes small after a few epochs of training and the other two regularization terms take over. Besides, this term is usually ignored as it is not positive-definite. This suggests that DAE is capable of learning sparse representation.

2.2.2 Contractive Auto-Encoder (CAE)

CAE [29] objective is given by

$$\mathcal{J}_{CAE} = \mathcal{J}_{AE} + \lambda \mathbb{E}_{\mathbf{x}} [\|J(\mathbf{x})\|_F^2] \quad (7)$$

where $J(\mathbf{x}) = \frac{\partial \mathbf{h}}{\partial \mathbf{x}}$ denotes the Jacobian matrix and the objective aims at minimizing the sensitivity of the hidden representation in input.

Remark 1. Let $\{\mathbf{W} \in \mathbb{R}^{m \times n}, \mathbf{b}_e \in \mathbb{R}^m\}$ represent the parameters of a Contractive Auto-Encoder (CAE) with $s_e(\cdot)$ activation function, squared loss or cross-entropy loss and regularization coefficient λ , at any point of training over data sampled from some distribution \mathcal{D} . Let $a_j := \mathbf{W}_j \mathbf{x} + b_{e_j}$ so that $h_j = s_e(a_j)$ corresponding to sample $\mathbf{x} \sim \mathcal{D}$. Then,

$$\mathcal{J}_{CAE} = \mathcal{J}_{AE} + \lambda \mathbb{E}_{\mathbf{x}} \left[\sum_{j=1}^m \left(\left(\frac{\partial h_j}{\partial a_j} \right)^2 \|\mathbf{W}_j\|_2^2 \right) \right] \quad (8)$$

Thus CAE regularization also has a form identical to the form suggested in corollary 2. Thus the hidden representation learned by CAE should also be sparse. In addition, since the first order regularization term in Higher order CAE (CAE+H) [28] is same as CAE, this suggests that CAE+H objective should have similar properties in term of sparsity.

2.2.3 Marginalized De-noising Auto-Encoder (mDAE)

mDAE [4] objective is given by:

$$\mathcal{J}_{mDAE} = \mathcal{J}_{AE} + \frac{1}{2} \mathbb{E}_{\mathbf{x}} \left[\sum_{i=1}^n \sigma_{\mathbf{x}_i}^2 \sum_{j=1}^m \frac{\partial^2 \ell}{\partial h_j^2} \left(\frac{\partial h_j}{\partial \tilde{x}_i} \right)^2 \right] \quad (9)$$

where $\sigma_{\mathbf{x}_i}^2$ denotes the corruption variance intended for the i^{th} input dimension. The authors of mDAE proposed this algorithm with the primary goal of speeding up the training of DAE by deriving an approximate form that omits the need to iterate over a large number of explicitly corrupted instances of every training sample.

Remark 2. Let $\{\mathbf{W} \in \mathbb{R}^{m \times n}, \mathbf{b}_e \in \mathbb{R}^m\}$ represent the parameters of a Marginalized De-noising Auto-Encoder (mDAE) with $s_e(\cdot)$ activation function, linear decoding, squared loss and $\sigma_{\mathbf{x}_i}^2 = \lambda \forall i \in \{1, \dots, n\}$, at any point of training over data sampled from some distribution \mathcal{D} . Let $a_j := \mathbf{W}_j \mathbf{x} + b_{e_j}$ so that $h_j = s_e(a_j)$ corresponding to sample $\mathbf{x} \sim \mathcal{D}$. Then,

$$\mathcal{J}_{mDAE} = \mathcal{J}_{AE} + \lambda \mathbb{E}_{\mathbf{x}} \left[\sum_{j=1}^m \left(\left(\frac{\partial h_j}{\partial a_j} \right)^2 \|\mathbf{W}_j\|_2^4 \right) \right] \quad (10)$$

Apart from justifying sparsity in the above AEs, these equivalences also expose the similarity between DAE, CAE and mDAE regularization as they all follow the form in corollary 2. Note how the goal of achieving invariance in hidden and original representation respectively in CAE and mDAE show up as a mere factor of weight length in their regularization in the case of linear decoding.

2.2.4 Sparse Auto-Encoder (SAE)

Sparse AEs are given by:

$$\mathcal{J}_{SAE} = \mathcal{J}_{AE} + \lambda \sum_{j=1}^m (\rho \log(\rho/\rho_j) + (1 - \rho) \log((1 - \rho)/(1 - \rho_j))) \quad (11)$$

where $\rho_j = \mathbb{E}_{\mathbf{x}}[h_j]$ and ρ is the desired average activation (typically close to 0). Thus SAE requires one additional parameter (ρ) that needs to be pre-determined. To make SAE follow our paradigm, we set $\rho = 0$ and thus tuning the value of λ would automatically enforce a balance between the final level of average sparsity and reconstruction error. Thus the SAE objective becomes

$$\mathcal{J}_{SAE} = \mathcal{J}_{AE} - \lambda \sum_{j=1}^m \log(1 - \rho_j) \quad (\text{when } \rho = 0) \quad (12)$$

Note for small values of ρ_j , $\log(1 - \rho_j) \approx -\rho_j$. Thus the above objective has a very close resemblance with sparse coding (equation 2, except that SC has a non-parametric encoder). On the other hand, the above regularization has a form as specified in corollary 1 which we have showed enforces sparsity. Thus, although it is expected of the SAE regularization to enforce sparsity from an intuitive standpoint, our results show that it indeed does so from a more theoretical perspective. Notice only Sigmoid is applicable to SAE in general due to the \log function. So we clip $\mathbb{E}_{\mathbf{x}}[h_j]$ at 1 during AE training process for applying other activations as well.

3 Improving Bias Gradient of ReLU with Rectified Softplus (ReS)

True sparsity (large number of hard zeros) is generally desired in feature representation for purposes like robustness, separability, compactness and performance. As discussed in section 2.1.1, while Maxout and Tanh do not satisfy the negative saturation property (and hence do not guarantee sparsity), ReLU, Softplus and Sigmoid satisfy the required properties (theorem 1) in general and thus encourage sparsity. However, the latter three activations each have some individual drawbacks. While ReLU does not have bias gradient which may lead to poor sparsity for regularizations in corollary 2 (eg. DAE, CAE, mDAE), Softplus and Sigmoid do not produce hard zeros.

As a by-product of the insights gained from our analysis, we propose an activation function *Rectified Softplus* (ReS), that overcomes the aforementioned drawbacks in individual activations (leading to better sparsity). We define ReS as $s_e(a_j) = \max(0, \log(\frac{1 + \exp^{a_j}}{2}))$. Note that ReS is a monotonically increasing convex function; thus theorem 1 applies.

Apart from the advantage of ReS over ReLU, Softplus and Sigmoid apparent from discussions above, one additional advantage of ReS (shared with ReLU and Softplus) over Sigmoid is its *large linear range* which helps in overcoming the problem of diminished weight gradients as against Sigmoid (due to saturation at 1) [6], leading to faster training.

4 Empirical Analysis and Observations

We use the following two datasets for our experiments:

1. MNIST [18]: It is a 10 class dataset of handwritten digit images (binary valued) of which 50,000 images are provided as train, 10,000 validation and 10,000 as test set.

2. CIFAR-10 [16]: It consists of 60000 32×32 real world (continuous valued) color images in 10 classes, with 6000 images per class. There are 50,000 train images and 10,000 test images. For CIFAR-10, we randomly crop 50,000 patches of size 8×8 (since CIFAR-10 has real world images) for training the auto-encoders.

Experimental Protocols: For all experiments, we use *RMS Prop* [31] for objective optimization, learning rate 0.001, pre-training epochs 100, batch size 50 and hidden units 1000 (for MNIST) and 500 (for CIFAR-10) unless specified otherwise. We train DAE, CAE, mDAE and SAE (using eq. 12) with the same aforementioned hyper-parameters for all the experiments. For regularization coefficient (σ^2), we use the values in the set $\{0.001, 0.1^2, 0.2^2, 0.3^2, 0.4^2, 0.5^2, 0.6^2, 0.7^2, 0.8^2, 0.9^2, 1.0\}$ for all models except DAE where σ^2 values represent the *variance* of Gaussian noise added. For all models and activation functions, we use squared loss and linear decoding. We initialize the bias to zeros and use normalized initialization [6] for weight vectors. Further, we subtract the mean from all the training samples.

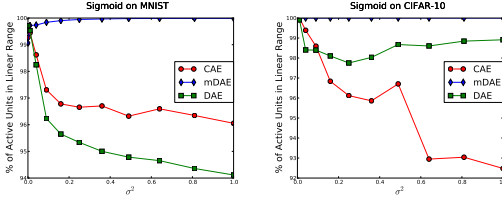


Figure 1: Fraction of activated units lying in linear range for AE models and datasets in case of Sigmoid. This suggests AEs only use the convex region of Sigmoid in practice justifying sparse representation in AEs.

4.1 Behaviour of Sigmoid Activation

We say that a Sigmoid unit has fired if $h_j \geq 0.1$ and we say a unit has saturated if $h_j \geq 0.9$. Thus a unit is in the linear region if $0.1 < h_j \leq 0.9$. We perform two types of experiments both of which confirm our argument in section 2.1.1 that AEs only make use of the linear range of Sigmoid activation and hence $\mathbb{E}_{\mathbf{x}} [\partial^2 h_j / \partial a_j^2] \geq 0$ for practical purposes which explains why Sigmoid learns sparse representation for DAE, CAE and mDAE (recall that corollary 1 always applies to Sigmoid; justifying sparsity for SAE):

1. $\mathbb{E}_{\mathbf{x}} [\partial^2 h_j / \partial a_j^2]$ vs. iterations: In order for corollary 2 to apply to Sigmoid, $\mathbb{E}_{\mathbf{x}} [\partial^2 h_j / \partial a_j^2] = \mathbb{E}_{\mathbf{x}} [h_j^2(1-h_j)^2(1-2h_j)]$ should be non-negative, which would lead sparsity to increase every iteration for the j^{th} unit. So we record the fraction of units for which $\mathbb{E}_{\mathbf{x}} [\partial^2 h_j / \partial a_j^2]$ is non-negative vs. training iterations for all the AE models. We found that this value is always close to 1 throughout the training iterations.

2. Percentage of active units in Linear Range: This is the ratio of the number of units in linear range to the number of units fired on percentage scale. The result as seen in figure 1 suggests more than 92% of activated units are in linear range for majority cases.

As a result of the above analysis, it is expected of Sigmoid activation to enforce low average activation fraction in the learned representation for all the four AE models. This is empirically verified in figures 3 and 4.

4.2 Sparsity vs. Regularization coefficient / Comparison of Activation functions

We analyze the effect of increasing regularization coefficient (σ^2) on the sparsity of representations learned by all the four AE models studied above on both the datasets using all activations⁴. As suggested by proposition 1, higher values of regularization coefficient should intuitively lead to lower average pre-activation, and based on our further analysis, it should ultimately lead to sparser representation. However, recall that the regularization in case of DAE, CAE and mDAE has the form $\sigma^2 \mathbb{E}_{\mathbf{x}} \left[\sum_{j=1}^m \left((\partial h_j / \partial a_j)^2 \|\mathbf{W}_j^t\|_2^p \right) \right]$. Note, only the term $(\partial h_j / \partial a_j)^2$ has effect on the gradient w.r.t the encoding bias \mathbf{b}_e (hence sparsity). Thus the term $\sigma^2 \|\mathbf{W}_j^t\|_2^p$ forms the *effective regularization coefficient* for the term $(\partial h_j / \partial a_j)^2$. Therefore, in order to exclusively analyze the trend of sparsity vs. regularization coefficient (σ^2), we constraint ⁵ $\|\mathbf{W}_j^t\|_2^p = 1$ and train all the AE objectives. The result on MNIST and CIFAR-10 can be seen in figure 3. Clearly, both Sigmoid and ReS have a stable decreasing trend for all the AE models. On the other hand, ReLU activation is sensitive towards CAE/mDAE. As suggested in section 2.1.1, an explanation for this observation **from the perspective of activation function** is that ReLU lacks gradient from the regularization w.r.t. the encoding bias \mathbf{b}_e , which is needed for regularizations in corollary 2 (eg. CAE, mDAE, DAE). So the bias gradient for ReLU in these cases entirely depends on the loss function. This can be verified in figure 2. Here, we compute the mean and standard-deviation of bias gradient (w.r.t. regularization) values across all units and samples during every training iteration⁶. We do the same for bias values as well. ReLU completely lacks bias gradient resulting in larger bias values (leading

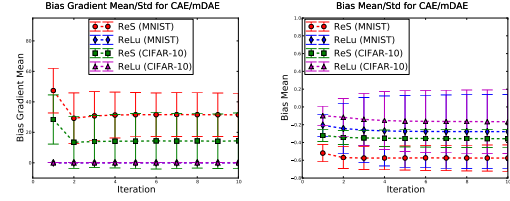


Figure 2: Bias Gradient mean (left) and Bias mean (right) for CAE/mDAE. ReLU lacks bias gradient, thus larger bias values. This results in poor sparsity for ReLU compared to ReS.

⁴We don't plot Softplus because its trend is very similar to Sigmoid. An explanation for this is that AEs use the convex region of Sigmoid, so both activations become similar in terms of their representational power.

⁵Note that CAE and mDAE objectives become identical in this case.

⁶Both bias gradient and thus bias values converge after the first 10 iterations.

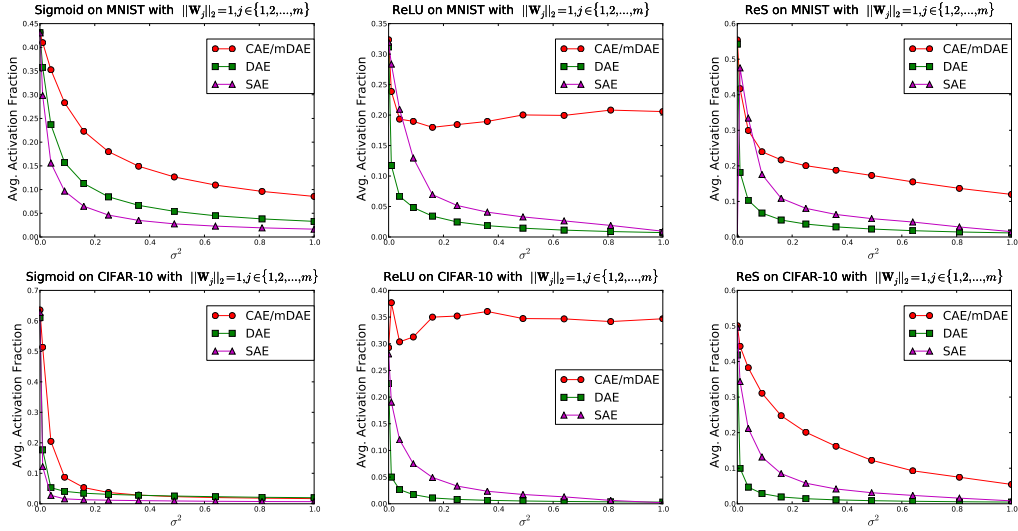


Figure 3: Results using Sigmoid, ReLU and ReS (left to right) activation functions on MNIST (top) and CIFAR-10 (bottom). Graphs show the trend of average activation fraction vs. regularization (σ^2) when weight vector are constrained to have unit length.

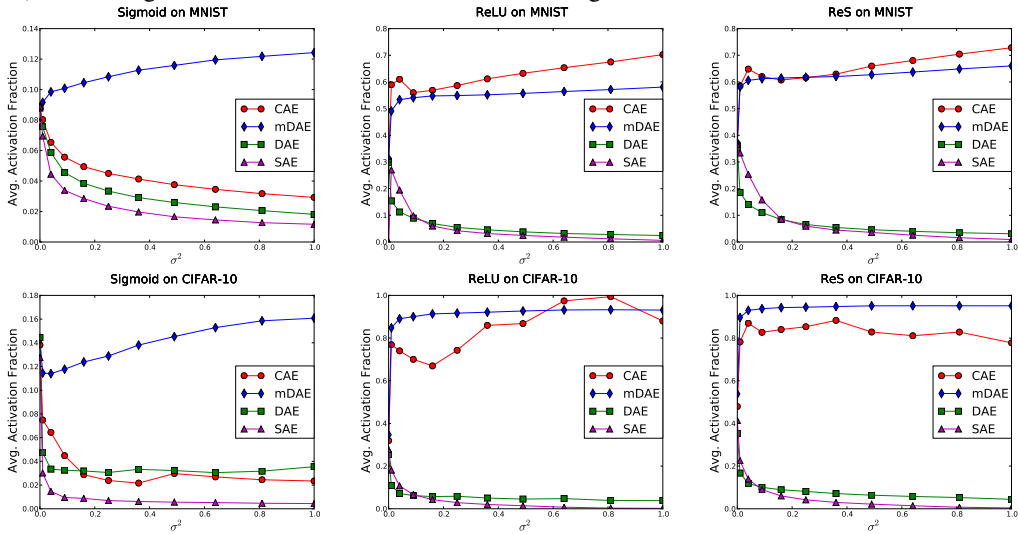


Figure 4: Results using Sigmoid, ReLU and ReS (left to right) activation functions on MNIST (top) and CIFAR-10 (bottom). Graphs show the trend of average activation fraction vs. regularization (σ^2) without any length constraint on weight vector.

to poor sparsity) compared to ReS. This result clearly confirms our analysis on ReLU and supports the proposed advantage of ReS.

4.3 Comparison of Auto-Encoder objectives

Here we are interested in analysing how sensitive different AE objectives are across various values of regularization coefficient (σ^2), activation functions and datasets. We do this in light of our analysis of the equivalent forms of AE objectives that we derive in section 2.2. So we train all the AE models without any extra constraint (as against section 4.2) and plot sparsity vs. σ^2 . The plots are shown in figure 4 for MNIST AND CIFAR-10. We find that the sparsity trend for both CAE and mDAE is sensitive to the value of regularization coefficient while that for DAE and SAE is stable and has a smooth decreasing trend. As already mentioned in section 4.2, a plausible explanation for this observation **from the perspective of AE objective function** is that $(\partial h_j / \partial a_j)^2$ is *effectively regularized* with the coefficient $\sigma^2 \|\mathbf{W}_j^t\|_2^p$ and hence σ^2 has a *non-linear* effect on the bias gradient.

4.3.1 Why is DAE less sensitive compared to CAE/mDAE?

The surprising part of the above experiments is that DAE has a stable sparsity trend (across different values of σ^2) for ReLU although DAE (similar to CAE, mDAE) has a regularization form given in corollary 2. The fact that ReLU practically does not generate bias gradients from this form of regularization brings our attention to an interesting possibility: ReLU is generating the positive bias gradient due to the first order regularization term in DAE. Recall that we marginalize out the first order term in DAE (during Taylor’s expansion, see proof in section 2.2.1) while taking expectation over all corrupted versions of a training sample. However, the mathematically equivalent objective of DAE obtained by this analytical marginalization is not what we optimize in practice. While optimizing with explicit corruption in a batch-wise manner, we indeed get a non-zero first order term, which does not vanish due to finite sampling (of corrupted versions); thus explaining sparsity for ReLU. We test this hypothesis by optimizing the explicit Taylor’s expansion of DAE (eDAE) with only the first order term on MNIST and CIFAR-10 using our standard experimental protocols:

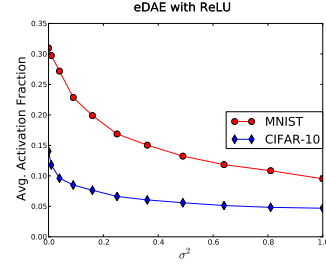


Figure 5: Activation fraction vs. σ^2 for eDAE.

$$\mathcal{J}_{eDAE} = \sum_{i=1}^N \ell(\mathbf{x}_i, f_d(f_e(\mathbf{x}_i))) + (\tilde{\mathbf{x}}_i - \mathbf{x}_i)^T \nabla_{\tilde{\mathbf{x}}_i} \ell \quad (13)$$

where $\tilde{\mathbf{x}}_i$ is a Gaussian corrupted version of \mathbf{x}_i and N denotes number of training samples. The activation fraction vs. corruption variance (σ^2) for eDAE is shown in figure 5 which confirms that the first order term contributes towards sparsity. On the other hand, both CAE and mDAE have regularizations with only second order terms, which as already discussed, do not generate bias gradients for ReLU and hence fail at sparsity. On a more general note, lower order terms (in Taylor’s expansion) of highly non-linear functions generally change slower (hence less sensitive) compared to higher order terms. In conclusion we find that explicit corruption may have advantages at times compared to marginalization because it captures the effect of both lower and higher order terms together.

4.4 Effect of True Sparsity on Supervised Performance

As mentioned in section 3, *true sparse* representation generally leads to better performance. On the same note, ReS overcomes the individual drawbacks of all the three activations– ReLU, Softplus and Sigmoid, thus encouraging true sparsity. Even though the focus of this paper is not on supervised evaluation on AEs, in order to test the effectiveness of *true sparsity* in the learned representations of AEs, we quantitatively analyse the robustness of the proposed activation function ReS against others on 8 different datasets. Apart from MNIST we use the following:

1. MNIST variants: This dataset ([17]) consists of 5 challenging variants of MNIST which include *basic*- a subsampled version, *bg_img*- randomly chosen images as background, *rot_bg_img* - rotated digits along with background images, *rot*- rotated version and *bg_rand*- random background pixels,. All these datasets have 10, 000 training images, 50, 000 test images and 2, 000 validation images.

2. Shape datasets: We use 2 shape datasets, *rect*- tall/short rectangles, and *rect_img*- rectangles with background images. While *rect_img* has 10, 000/50, 000/2, 000 train/test/validation images, *rect* has 1, 000/50, 000/200 train/test/validation images. More details can be found in [17].

Since our paper focuses on analysing unsupervised representation learning using single layer AEs, we train different AE models and use them as feature extractors, *i.e.*, **we do not fine-tune** the weight vectors of the AEs. The hyper-parameters for training all the AEs are chosen on the validation set. These include the learning rate for pre-training (candidate set $\{0.0001, 0.0005, 0.001, 0.005, 0.01\}$) and regularization coefficient σ^2 (candidate set $\{0.001, 0.1^2, 0.3^2, 0.5^2\}$). Finally, we use linear SVM for classification using the extracted features with penalty C from candidate set $\{0.01, 0.1, 1, 10\}$. The test errors chosen on the best validation performance for MNIST can be seen in table 1. We find a couple of interesting observations:

1) ReLU generally performs better than Sigmoid/Softplus for DAE/SAE as compared with CAE/mDAE across datasets. We believe this is due to a trade-off between better *true sparsity* and bias gradient. ReLU is *potentially* capable of generating hard zeros but has weak bias gradient for CAE/mDAE, while Sigmoid and Softplus exhibit the exact opposite behaviour for all AE models. On the other hand, ReLU has no bias gradient problem for DAE/SAE.

- 2) Sigmoid and Softplus have relatively similar performance across AE models and datasets.
- 3) Finally, ReS retains the benefits of all– ReLU, Sigmoid and Softplus; thus produces performance at par (or better) with the best performing activation for all AE models consistently. In particular, ReS consistently outperforms ReLU by generating stronger bias gradient.

MNIST	CAE	mDAE	DAE	SAE	basic	CAE	mDAE	DAE	SAE
ReLU	2.1	1.57	1.63	1.93	ReLU	3.41	2.97	3.81	3.42
Sigmoid	1.94	1.48	1.82	3.44	Sigmoid	3.71	3.11	3.6	5.46
Softplus	1.83	1.48	1.68	2.91	Softplus	3.73	2.96	3.59	6.60
ReS	1.86	1.53	1.41	1.67	ReS	3.04	3.16	3.10	4.12
bg_img	CAE	mDAE	DAE	SAE	rot_bg_img	CAE	mDAE	DAE	SAE
ReLU	20.15	19.52	17.9	22.81	ReLU	54.48	53.05	52.22	57.91
Sigmoid	25.09	21.20	21.58	27.72	Sigmoid	59.88	54.8	55.25	60.63
Softplus	24.43	20.06	21.1	27.55	Softplus	58.12	53.75	57.26	62.60
ReS	18.37	18.67	18.06	21.41	ReS	50.88	52.40	51.65	57.41
rot	CAE	mDAE	DAE	SAE	bg_rand	CAE	mDAE	DAE	SAE
ReLU	19.39	17.19	21.61	22.67	ReLU	18.76	18.41	14.68	20.66
Sigmoid	19.63	14.87	17.16	27.48	Sigmoid	18.01	14.37	15.23	18.55
Softplus	17.40	16.32	16.29	28.67	Softplus	15.82	14.11	15.51	16.45
ReS	16.29	16.0	17.06	21.04	ReS	16.66	16.05	15.35	20.16
rect	CAE	mDAE	DAE	SAE	rect_img	CAE	mDAE	DAE	SAE
ReLU	0.46	0.28	0.08	0.18	ReLU	23.38	22.44	22.99	23.79
Sigmoid	0.84	0.89	0.40	1.91	Sigmoid	25.73	23.26	22.91	28.26
Softplus	0.54	0.42	0.14	0.81	Softplus	23.3	22.56	22.19	26.36
ReS	0.20	0.23	0.04	0.18	ReS	23.13	22.2	23.05	23.96

Table 1: Classification performance on various datasets using different activation functions and single layer auto-encoder models without fine-tuning.

5 Conclusion

Inspired from the fact that neurons in brain exhibit sparse distributed behavior, we establish a connection between auto-encoders and sparse representation. Our contribution is multi-fold, we show: a) AE regularizations with positive encoding bias gradient encourage low pre-activation values (proposition 1); b) monotonically increasing convex activation functions with negative saturation at zero encourage sparsity for such regularizations (theorem 1) and that multiple existing activations satisfy them; c) existing AEs have regularizations of the form suggested in corollary 1 and 2, justifying why they learn sparse representation. d) Based on these insights, we propose a new activation function (ReS in section 3) which overcomes the individual drawbacks of existing activations in terms of sparsity leading to better empirical performance.

On the empirical side, a) we find that AEs only use the convex region of Sigmoid (section 4.1) which justifies learning sparse representation using this activation; b) ReLU leads to poor sparsity for CAE and mDAE due to the absence of bias gradients(section 4.2) compared with Sigmoid and ReS; c) DAE and SAE are less sensitive to regularization coefficient compared with CAE and mDAE (section 4.3) in terms of sparsity; d) explicit corruption (*eg.* DAE) may have advantages over marginalizing it out (*eg.* mDAE, see section 4.3.1) because it captures both first and second order effects. In conclusion, our analysis combined together yields new insights into AEs and provides novel tools for analyzing existing (and new) regularization/activation functions that help predicting whether the resulting AE learns sparse representations.

References

- [1] Yoshua Bengio. Learning deep architectures for AI. *Found. Trends Mach. Learn.*, 2(1):1–127, January 2009.
- [2] Yoshua Bengio, Grégoire Mesnil, Yann Dauphin, and Salah Rifai. Better mixing via deep representations. In *ICML*, pages 552–560, 2013.
- [3] H. Bourlard and Y. Kamp. Auto-association by multilayer perceptrons and singular value decomposition. *Biological Cybernetics*, 59(4-5):291–294, 1988.

- [4] Minmin Chen, Kilian Q. Weinberger, Fei Sha, and Yoshua Bengio. Marginalized denoising auto-encoders for nonlinear representations. In *ICML*, pages 1476–1484, 2014.
- [5] Adam Coates and Andrew Y. Ng. The importance of encoding versus training with sparse coding and vector quantization. In *ICML*, pages 921–928, 2011.
- [6] Xavier Glorot and Yoshua Bengio. Understanding the difficulty of training deep feedforward neural networks. In *AISTATS*, 2010.
- [7] Xavier Glorot, Antoine Bordes, and Yoshua Bengio. Deep sparse rectifier neural networks. In *AISTATS*, pages 315–323, 2011.
- [8] Ian J. Goodfellow, David Warde-Farley, Mehdi Mirza, Aaron C. Courville, and Yoshua Bengio. Maxout networks. In *ICML*, pages 1319–1327, 2013.
- [9] Robert Hecht-Nielsen. Theory of the backpropagation neural network. In *Neural Networks, 1989. IJCNN., International Joint Conference on*, pages 593–605. IEEE, 1989.
- [10] Geoffrey Hinton, Nitish Srivastava, Alex Krizhevsky, Ilya Sutskever, and Ruslan Salakhutdinov. Improving neural networks by preventing co-adaptation of feature detectors. *CoRR*, abs/1207.0580, 2012.
- [11] Geoffrey E Hinton. Distributed representations. 1984.
- [12] D. H. Hubel and T. N. Wiesel. Receptive fields of single neurones in the cat’s striate cortex. *The Journal of physiology*, 148:574–591, October 1959.
- [13] Alumit Ishai, Leslie Ungerleider, Alex Martin, Jennifer Schouten, and James Haxby. Distributed representation of objects in the human ventral visual pathway. *Proc Natl Acad Sci*, 96(16):9379–9384, 1999.
- [14] Koray Kavukcuoglu and Yann Lecun. Fast inference in sparse coding algorithms with applications to object recognition. Technical report, Courant Institute, NYU, 2008.
- [15] Koray Kavukcuoglu, Marc’Aurelio Ranzato, and Yann LeCun. Fast inference in sparse coding algorithms with applications to object recognition. *arXiv preprint arXiv:1010.3467*, 2010.
- [16] Alex Krizhevsky. Learning Multiple Layers of Features from Tiny Images. Technical report, 2009.
- [17] Hugo Larochelle, Dumitru Erhan, Aaron C. Courville, James Bergstra, and Yoshua Bengio. An empirical evaluation of deep architectures on problems with many factors of variation. In *ICML*, pages 473–480, 2007.
- [18] Yann Lecun and Corinna Cortes. The MNIST database of handwritten digits.
- [19] Honglak Lee, Chaitanya Ekanadham, and Andrew Y. Ng. Sparse deep belief net model for visual area v2. In *Advances in Neural Information Processing Systems 20*. MIT Press, 2008.
- [20] Jun Li, Wei Luo, Jian Yang, and Xiaotong Yuan. Why does the unsupervised pretraining encourage moderate-sparseness? *CoRR*, abs/1312.5813, 2013.
- [21] Richard P Lippmann. An introduction to computing with neural nets. *ASSP, IEEE*, 4(2):4–22, 1987.
- [22] Alireza Makhzani and Brendan Frey. k-sparse autoencoders. *CoRR*, abs/1312.5663, 2013.
- [23] Roland Memisevic, Kishore Reddy Konda, and David Krueger. Zero-bias autoencoders and the benefits of co-adapting features. In *ICLR*, 2014.
- [24] Vinod Nair and Geoffrey E. Hinton. Rectified linear units improve restricted boltzmann machines. In *ICML*, pages 807–814, 2010.
- [25] Andrew Ng. Sparse autoencoder. *CSE294 Lecture notes*, 2011.
- [26] Bruno A. Olshausen and David J. Fieldt. Sparse coding with an overcomplete basis set: a strategy employed by v1. *Vision Research*, 37:3311–3325, 1997.
- [27] Karalyn Patterson, Peter Nestor, and Timothy Rogers. Where do you know what you know? the representation of semantic knowledge in the human brain. *Nature Rev. Neuroscience*, 8(12):976–987, 2007.
- [28] Salah Rifai, Grégoire Mesnil, Pascal Vincent, Xavier Muller, Yoshua Bengio, Yann Dauphin, and Xavier Glorot. Higher order contractive auto-encoder. In *ECML/PKDD*, pages 645–660, 2011.
- [29] Salah Rifai, Pascal Vincent, Xavier Muller, Xavier Glorot, and Yoshua Bengio. Contractive auto-encoders: Explicit invariance during feature extraction. In *ICML*, pages 833–840, 2011.
- [30] David E. Rumelhart, Geoffrey E. Hinton, and Ronald J. Williams. Learning representations by back-propagating errors. *Nature*, pages 533–536, 1986.
- [31] T Tieleman and G Hinton. Lecture 6.5-rmsprop: Divide the gradient by a running average of its recent magnitude. In *COURSERA: Neural Networks for Machine Learning*, 2012.
- [32] Pascal Vincent, Hugo Larochelle, Yoshua Bengio, and Pierre-Antoine Manzagol. Extracting and composing robust features with denoising autoencoders. In *ICML*, pages 1096–1103, 2008.
- [33] J. Wright, A.Y. Yang, A. Ganesh, S.S. Sastry, and Yi Ma. Robust face recognition via sparse representation. *IEEE TPAMI*, 31(2):210–227, Feb. 2009.
- [34] Jianchao Yang, Kai Yu, Yihong Gong, and Thomas Huang. Linear spatial pyramid matching using sparse coding for image classification. In *CVPR*, pages 1794–1801, 2009.

A1 Supplementary Material

A1.1 Supplementary Proofs

Proposition 1. Let $\{\mathbf{W}^t \in \mathbb{R}^{m \times n}, \mathbf{b}_e^t \in \mathbb{R}^m\}$ be the parameters of a regularized auto-encoder ($\lambda > 0$)

$$\mathcal{J}_{RAE} = \mathcal{J}_{AE} + \lambda \mathcal{R}(\mathbf{W}, \mathbf{b}_e) \quad (14)$$

at training iteration t with regularization term $\mathcal{R}(\mathbf{W}, \mathbf{b}_e)$, activation function $s_e(\cdot)$ and define pre-activation $a_j^t = \mathbf{W}_j^t \mathbf{x} + b_{e_j}^t$ (thus $h_j^t = s_e(a_j^t)$). If $\frac{\partial \mathcal{R}}{\partial b_{e_j}} > 0$, where $j \in \{1, 2, \dots, m\}$, **and** $\mathbb{E}_{\mathbf{x}}[\mathbf{x}] = \mathbf{0}$, **then** updating $\{\mathbf{W}^t, \mathbf{b}_e^t\}$ along the negative gradient of $\lambda \mathcal{R}$, results in $\mathbb{E}_{\mathbf{x}}[a_j^{t+1}] < \mathbb{E}_{\mathbf{x}}[a_j^t]$ **and** $\text{var}[a_j^{t+1}] \leq \lambda_x^2 \|\mathbf{W}_j^{t+1}\|^2$ **for all** $t \geq 0$. Here λ_x^2 denotes the maximum eigenvalues of $\mathbb{E}_{\mathbf{x}}[\mathbf{x}\mathbf{x}^T]$.

Proof. At iteration $t + 1$,

$$a_j^{t+1} = a_j^t - \eta \lambda \frac{\partial \mathcal{R}}{\partial \mathbf{W}_j} \mathbf{x} - \eta \lambda \frac{\partial \mathcal{R}}{\partial b_{e_j}} \quad (15)$$

for any step size η . Thus

$$\mathbb{E}_{\mathbf{x}}[a_j^{t+1}] = \mathbb{E}_{\mathbf{x}}[a_j^t] - \eta \lambda \frac{\partial \mathcal{R}}{\partial b_{e_j}} \quad (16)$$

Thus if $\frac{\partial \mathcal{R}}{\partial b_{e_j}} > 0$, then $\mathbb{E}_{\mathbf{x}}[a_j^{t+1}] < \mathbb{E}_{\mathbf{x}}[a_j^t]$.

Finally, $\text{var}[a_j^{t+1}] = \mathbb{E}_{\mathbf{x}}[a_j^{t+1} - \mathbb{E}_{\mathbf{x}}[a_j^{t+1}]]^2 = \mathbb{E}_{\mathbf{x}}[\mathbf{W}_j^{t+1} \mathbf{x}]^2 \leq \lambda_x^2 \|\mathbf{W}_j^{t+1}\|^2$ \square

Corollary 1. If s_e is a monotonically increasing activation function **and** $\mathbb{E}_{\mathbf{x}}[\mathbf{x}] = \mathbf{0}$, **then** updating $\{\mathbf{W}^t, \mathbf{b}_e^t\}$ along the negative gradient of $\mathcal{R} = \sum_{j=1}^m f(\mathbb{E}_{\mathbf{x}}[h_j])$, results in $\mathbb{E}_{\mathbf{x}}[a_j^{t+1}] \leq \mathbb{E}_{\mathbf{x}}[a_j^t]$ **and** $\text{var}[a_j^{t+1}] \leq \lambda_x^2 \|\mathbf{W}_j^{t+1}\|^2$ **for all** $t \geq 0$. Here $f(\cdot)$ is any monotonically increasing function.

Proof. We need one additional argument other than proposition 1. $\frac{\partial \mathcal{R}}{\partial b_{e_j}} = \frac{\partial f(\mathbb{E}_{\mathbf{x}}[h_j])}{\partial \mathbb{E}_{\mathbf{x}}[h_j]} \mathbb{E}_{\mathbf{x}} \left[\frac{\partial h_j}{\partial a_j} \right]$. Since both $s_e(\cdot)$ and $f(\cdot)$ are monotonically increasing functions, $\frac{\partial \mathcal{R}}{\partial b_{e_j}} \geq 0$ in all cases. \square

Corollary 2. If $s_e(\cdot)$ is a monotonically increasing convex activation function **and** $\mathbb{E}_{\mathbf{x}}[\mathbf{x}] = \mathbf{0}$, **then** updating $\{\mathbf{W}^t, \mathbf{b}_e^t\}$ along the negative gradient of $\mathcal{R} = \mathbb{E}_{\mathbf{x}} \left[\sum_{j=1}^m \left(\left(\frac{\partial h_j}{\partial a_j} \right)^q \|\mathbf{W}_j^t\|_2^p \right) \right]$, $q \in \mathbb{N}$, $p \in \mathbb{W}$, results in $\mathbb{E}_{\mathbf{x}}[a_j^{t+1}] \leq \mathbb{E}_{\mathbf{x}}[a_j^t]$ **and** $\text{var}[a_j^{t+1}] \leq \lambda_x^2 \|\mathbf{W}_j^{t+1}\|^2$ **for all** $t \geq 0$.

Proof. We need one additional argument other than proposition 1. $\frac{\partial \mathcal{R}}{\partial b_{e_j}} = \mathbb{E}_{\mathbf{x}} \left[q \left(\frac{\partial h_j}{\partial a_j} \right)^{q-1} \frac{\partial^2 h_j}{\partial a_j^2} \frac{\partial a_j}{\partial b_{e_j}} \|\mathbf{W}_j^t\|_2^p \right]$. Since $s_e(\cdot)$ is a monotonically increasing convex function, both $\frac{\partial^2 s_e(a_j)}{\partial a_j^2} \geq 0$ and $\frac{\partial s_e(a_j)}{\partial a_j} \geq 0 \forall a_j \in \mathbb{R}$. Finally, $\frac{\partial a_j}{\partial b_{e_j}} = 1$ by definition. Thus $\frac{\partial \mathcal{R}}{\partial b_{e_j}} \geq 0$ in all cases. \square

Theorem 1. Let p_j^t denote a lower bound of $\Pr(h_j^t \leq \delta_{\min})$ at iteration t and $s_e(\cdot)$ be a monotonically increasing function. Extending the argument of proposition 1, if $\|\mathbf{W}_j^t\|_2$ is upper bounded independent of λ **then** $\exists S \subseteq \mathbb{R}^+$ **and** $\exists T_{\min} \in \mathbb{N}$ **such that** $p_j^{t+1} \geq p_j^t \forall \lambda \in S, T_{\min} \leq t \leq T_{\max}$ for any fixed $T_{\max} \in \mathbb{N}$.

Proof. From proposition 1, $\mathbb{E}[a_j^{t+1}] < \mathbb{E}[a_j^t] \forall t \geq 0$. Define a_{\min} such that $\delta_{\min} = \max_{a_{\min}} s_e(a_{\min})$. Thus $\exists T_{\min} \in \mathbb{N}$, such that $\forall t \geq T_{\min}, \mathbb{E}[a_j^t] < a_{\min}$. Then in the case of monotonically increasing activation functions, using Chebyshev's bound,

$$\begin{aligned} \Pr(h_j^t \leq \delta_{\min}) &= \Pr(a_j^t \leq a_{\min}) \geq \Pr(|a_j^t - \mathbb{E}[a_j^t]| \leq a_{\min} - \mathbb{E}[a_j^t]) \\ &\geq 1 - \frac{\text{var}[a_j^t]}{(a_{\min} - \mathbb{E}[a_j^t])^2} \end{aligned} \quad (17)$$

Thus $p_j^t := 1 - \frac{\text{var}[a_j^t]}{(a_{\min} - \mathbb{E}[a_j^t])^2}$ lower bounds $\Pr(h_j^t \leq \delta_{\min}) \forall t \geq T_{\min}$. Now consider the difference

$$D(t) := \frac{\text{var}[a_j^{t+1}]}{(a_{\min} - \mathbb{E}[a_j^{t+1}])^2} - \frac{\text{var}[a_j^t]}{(a_{\min} - \mathbb{E}[a_j^t])^2} \quad (18)$$

and recall that

$$\mathbb{E}_{\mathbf{x}} [a_j^{t+1}] = \mathbb{E}_{\mathbf{x}} [a_j^t] - \eta\lambda \frac{\partial \mathcal{R}}{\partial b_{e_j}} \quad (19)$$

where both the step size η and $\frac{\partial \mathcal{R}}{\partial b_{e_j}}$ are positive. Thus, since $\text{var}[a_j] \leq \lambda_x^2 \|\mathbf{W}_j^t\|^2$, we can always choose a fixed $S \subseteq \mathbb{R}^+$ such that $D(t) < 0 \forall \lambda \in S$ and $T_{\min} \leq t \leq T_{\max}$. \square

Theorem 2. Let $\{\mathbf{W}, \mathbf{b}_e\}$ represent the parameters of a DAE with squared loss, linear decoding, and i.i.d. Gaussian corruption with zero mean and σ^2 variance, at any point of training over data sampled from distribution \mathcal{D} . Let $a_j := \mathbf{W}_j \mathbf{x} + b_{e_j}$ so that $h_j = s_e(a_j)$ corresponding to sample $\mathbf{x} \sim \mathcal{D}$. Then,

$$\begin{aligned} \mathcal{J}_{DAE} = \mathcal{J}_{AE} + \sigma^2 \mathbb{E}_{\mathbf{x}} \left[\sum_{j=1}^m \left(\left(\frac{\partial h_j}{\partial a_j} \right)^2 \|\mathbf{W}_j\|_2^4 \right) + \sum_{\substack{j,k=1 \\ j \neq k}}^m \left(\frac{\partial h_j}{\partial a_j} \frac{\partial h_k}{\partial a_k} (\mathbf{W}_j^T \mathbf{W}_k)^2 \right) \right] \\ + \sum_{i=1}^n \left((\mathbf{b}_d + \mathbf{W}^T \mathbf{h} - \mathbf{x})^T \mathbf{W}^T \left(\frac{\partial^2 \mathbf{h}}{\partial \mathbf{a}^2} \odot \mathbf{W}^i \odot \mathbf{W}^i \right) \right) + o(\sigma^2) \end{aligned} \quad (20)$$

where $\frac{\partial^2 \mathbf{h}}{\partial \mathbf{a}^2} \in \mathbb{R}^m$ is the element-wise 2nd derivative of \mathbf{h} w.r.t. \mathbf{a} and \odot is element-wise product.

Proof. Using 2nd order Taylor's expansion of the loss function, we get

$$\ell(\mathbf{x}, f_d(f_e(\tilde{\mathbf{x}}))) = \ell(\mathbf{x}, f_d(f_e(\mu_{\mathbf{x}}))) + (\tilde{\mathbf{x}} - \mu_{\mathbf{x}})^T \nabla_{\tilde{\mathbf{x}}} \ell + \frac{1}{2} (\tilde{\mathbf{x}} - \mu_{\mathbf{x}})^T \nabla_{\tilde{\mathbf{x}}}^2 \ell (\tilde{\mathbf{x}} - \mu_{\mathbf{x}}) + o(\sigma^2) \quad (21)$$

Since the corruption process is Gaussian with zero mean, taking the expectation of this approximation yields

$$\mathbb{E}[\ell(\mathbf{x}, f_d(f_e(\tilde{\mathbf{x}})))] = \mathbb{E}[\ell(\mathbf{x}, f_d(f_e(\mu_{\mathbf{x}})))] + \frac{1}{2} \text{tr}(\Sigma_{\tilde{\mathbf{x}}} \nabla_{\tilde{\mathbf{x}}}^2 \ell) + o(\sigma^2) \quad (22)$$

where $\Sigma_{\tilde{\mathbf{x}}} := \mathbb{E}[(\tilde{\mathbf{x}} - \mu_{\mathbf{x}})(\tilde{\mathbf{x}} - \mu_{\mathbf{x}})^T]$. Since the corruption is i.i.d., assume the covariance $\Sigma_{\tilde{\mathbf{x}}} = \sigma^2 \mathbf{I}$, where \mathbf{I} is the identity matrix.

Thus we can rewrite equation (22) as

$$\mathcal{J}_{DAE} = \mathcal{J}_{AE} + \frac{1}{2} \sigma^2 \sum_{i=1}^n \frac{\partial^2 \ell}{\partial \tilde{x}_i^2} + o(\sigma^2) \quad (23)$$

Expanding the second order term in the above equation, we get

$$\frac{\partial^2 \ell}{\partial \tilde{x}_i^2} = \frac{\partial \mathbf{h}^T}{\partial \tilde{x}_i} \frac{\partial^2 \ell}{\partial \mathbf{h}^2} \frac{\partial \mathbf{h}}{\partial \tilde{x}_i} + \frac{\partial \ell^T}{\partial \mathbf{h}} \frac{\partial^2 \mathbf{h}}{\partial \tilde{x}_i^2} \quad (24)$$

For linear decoding and squared loss,

$$\frac{\partial \ell^T}{\partial \mathbf{h}} \frac{\partial^2 \mathbf{h}}{\partial \tilde{x}_i^2} = \sum_{i=1}^n \left((\mathbf{b}_d + \mathbf{W}^T \mathbf{h} - \mathbf{x})^T \mathbf{W}^T \left(\frac{\partial^2 \mathbf{h}}{\partial \mathbf{a}^2} \odot \mathbf{W}^i \odot \mathbf{W}^i \right) \right) \quad (25)$$

where $\frac{\partial^2 \mathbf{h}}{\partial \mathbf{a}^2} \in \mathbb{R}^m$ is the element-wise 2^{nd} derivative of \mathbf{h} w.r.t. \mathbf{a} , \odot represents element-wise product and \mathbf{W}^i denotes the i^{th} column of \mathbf{W} . Let vector $\mathbf{d}_h \in \mathbb{R}^m$ be defined such that $d_{h_j} = \frac{\partial h_j}{\partial a_j} \forall j \in \{1, 2, \dots, m\}$. Then,

$$\sum_{i=1}^n \frac{\partial \mathbf{h}^T}{\partial \tilde{\mathbf{x}}_i} \frac{\partial^2 \ell}{\partial \mathbf{h}^2} \frac{\partial \mathbf{h}}{\partial \tilde{\mathbf{x}}_i} = 2 \sum_{j=1}^n \sum_{k=1}^n ((\mathbf{d}_h \odot (\mathbf{W})^j)^T (\mathbf{W})^k)^2 \quad (26)$$

where $(\mathbf{W})^j$ represents the j^{th} column of \mathbf{W} and \odot denotes element-wise product. Let $\mathbf{D}_h = \text{diag}(\mathbf{d}_h)$. Then,

$$\sum_{j=1}^n \sum_{k=1}^n ((\mathbf{d}_h \odot (\mathbf{W})^j)^T (\mathbf{W})^k)^2 = \|(\mathbf{D}_h \mathbf{W})^T \mathbf{W}\|_F^2 \quad (27)$$

Finally, using the cyclic property of trace operator, we get, $\|(\mathbf{D}_h \mathbf{W})^T \mathbf{W}\|_F^2 = \text{tr}(\mathbf{W}^T \mathbf{D}_h \mathbf{W} \mathbf{W}^T \mathbf{D}_h \mathbf{W}) = \text{tr}(\mathbf{D}_h \mathbf{W} \mathbf{W}^T \mathbf{D}_h \mathbf{W} \mathbf{W}^T)$. Thus DAE objective becomes,

$$\begin{aligned} \mathcal{J}_{DAE} &= \mathcal{J}_{AE} + \sigma^2 \mathbb{E}_{\mathbf{x}}[\text{tr}(\mathbf{D}_h \mathbf{W} \mathbf{W}^T \mathbf{D}_h \mathbf{W} \mathbf{W}^T)] + \\ &\sum_{i=1}^n \left((\mathbf{b}_d + \mathbf{W}^T \mathbf{h} - \mathbf{x})^T \mathbf{W}^T \left(\frac{\partial^2 \mathbf{h}}{\partial \mathbf{a}^2} \odot \mathbf{W}^i \odot \mathbf{W}^i \right) \right) + o(\sigma^2) \end{aligned} \quad (28)$$

Upon expansion of the second term above, we get the final form. \square

Remark 3. Let $\{\mathbf{W} \in \mathbb{R}^{m \times n}, \mathbf{b}_e \in \mathbb{R}^m\}$ represent the parameters of a Marginalized De-noising Auto-Encoder (mDAE) with $s_e(\cdot)$ activation function, linear decoding, squared loss and $\sigma_{\mathbf{x}_i}^2 = \lambda \forall i \in \{1, \dots, n\}$, at any point of training over data sampled from some distribution \mathcal{D} . Let $a_j := \mathbf{W}_j \mathbf{x} + b_{e_j}$ so that $h_j = s_e(a_j)$ corresponding to sample $\mathbf{x} \sim \mathcal{D}$. Then,

$$\mathcal{J}_{mDAE} = \mathcal{J}_{AE} + \lambda \mathbb{E}_{\mathbf{x}} \left[\sum_{j=1}^m \left(\left(\frac{\partial h_j}{\partial a_j} \right)^2 \|\mathbf{W}_j\|_2^4 \right) \right] \quad (29)$$

Proof. For linear decoding and squared loss, $\frac{\partial^2 \ell}{\partial h_j^2} = 2 \|\mathbf{W}_j\|_2^2$ and $\frac{\partial h_j}{\partial \mathbf{x}_i} = \frac{\partial h_j}{\partial a_j} W_{ji}$. Thus

$$\begin{aligned} \frac{1}{2} \sum_{i=1}^n \sigma_{\mathbf{x}_i}^2 \sum_{j=1}^m \frac{\partial^2 \ell}{\partial h_j^2} \left(\frac{\partial h_j}{\partial \tilde{\mathbf{x}}_i} \right)^2 &= \sum_{i=1}^n \lambda \sum_{j=1}^m \|\mathbf{W}_j\|_2^2 \left(\frac{\partial h_j}{\partial a_j} W_{ji} \right)^2 \\ &= \lambda \sum_{j=1}^m \|\mathbf{W}_j\|_2^2 \left(\frac{\partial h_j}{\partial a_j} \right)^2 \sum_{i=1}^n W_{ji}^2 = \lambda \sum_{j=1}^m \left(\frac{\partial h_j}{\partial a_j} \right)^2 \|\mathbf{W}_j\|_2^4 \end{aligned} \quad (30)$$

\square